Research article

Development of a new type of passively adaptive compliant gripper

Dalibor Petković and Nenad D. Pavlović
Faculty of Mechanical Engineering, Department of Mechatronics, University of Niš, Niš, Serbia

Shahaboddin Shamshirband
Department of Computer System and Technology, Faculty of Computer Science and Information Technology, University of Malaya, Kuala Lumpur, Malaysia and
Department of Computer Science, Islamic Azad University (IAU), Chalous, Iran, and

Nor Badrul Anuar
Department of Computer System and Technology, Faculty of Computer Science and Information Technology, University of Malaya, Kuala Lumpur, Malaysia

Abstract

Purpose – Passively compliant underactuated mechanisms are one way to obtain the gripper which could accommodate to any irregular and sensitive grasping object. The purpose of the underactuation is to use less active inputs than the number of degrees of freedom of the gripper mechanism to drive the open and close motion of the gripper. Another purpose of underaction is to reduce the number of control variables.

Design/methodology/approach – The underactuation can morph shapes of the gripper to accommodate different objects. As a result, the underactuated grippers require less complex control algorithms. The fully compliant mechanism has multiple degrees of freedom and can be considered as an underactuated mechanism.

Findings – This paper presents a new design of the adaptive underactuated compliant gripper with distributed compliance. The optimal topology of the gripper structure was obtained by optimality criteria method using mathematical programming technique. Afterwards, the obtained model was improved by iterative finite element optimization procedure. The gripper was constructed entirely of silicon rubber.

Originality/value – The main points of this paper are the explanation of the development and production of the new compliant gripper structure.

Keywords Robots, Grippers, Mechanisms

Paper type Research paper

1. Introduction

A system is said to be adaptive if it has the capacity for adaptation, i.e. the ability to respond successfully to a new situation. An adaptive (robotic) mechanical system is an adaptive system in which the ability to adapt to new external situations relies strictly on mechanical properties. In other words, an adaptive mechanical system is one in which some form of intelligence is embedded into the mechanics. In such a system, no sensors or complex controllers are required to perform the main task since the mechanical system itself will provide the required adaptive behavior.

Significant efforts have been made to find designs simple enough to be easily built and controlled, in order to obtain practical systems. To overcome the limited success of the early designs (mainly due to the cost of the control architecture needed for complex mechanical systems with often more than ten actuators plus many sensors), a special emphasis has been placed on the reduction of the number of degrees of freedom, thereby decreasing the number of actuators. The strategy for reducing the number of actuators while keeping the hand capability to adapt its shape to the grasped object (to increase the number of contact points) is referred to as underactuation (Birglen *et al.*, 2008; Doria and Birglen, 2009). Carrozza *et al.* (2004), Montambault and Gosselin (2001), Fukaya *et al.* (2000) and Birglen (2011) show that underactuation allows the reproduction of most of the grasping behaviors of the human hand, without augmenting the mechanical and

The current issue and full text archive of this journal is available at
www.emeraldinsight.com/0143-991X.htm

Industrial Robot: An International Journal
40/6 (2013) 610–623

[DOI 10.1108/IR-12-2012-452]

The first two authors would like to acknowledge Steutel *et al.* (2010) who inspire the development of the gripper design. This paper is supported by Project Grant TP35005 "Research and development of new generation wind turbines of high-energy efficiency" (2011-2014) financed by Ministry of Education, Science and Technological Development, Republic of Serbia. The last author work was partially funded by the University of Malaya under Grant RP005A-13ICT.

Received: 26 December 2012
Revised: 9 May 2013
Accepted: 10 May 2013

control complexity. These papers focus on an innovative approach to achieve enhanced grasping functionality based on underactuated mechanisms.

A mechanism is said to be underactuated when it has fewer actuators than degrees of freedom. In order to achieve this goal, passive elastic elements are used. They are small, light and simple and lead to a reduction of the number of actuators, which is the main advantage of underactuation. The elastic elements are useful for keeping the finger from incoherent motion, but when the grasp sequence is complete, they still oppose the actuation. Thus, the elastic elements should be designed with the smallest stiffness possible, however, sufficient to keep the finger from collapsing. The transmission mechanism used to achieve such a property must be adaptive, i.e. when one or more fingers are blocked, the remaining finger(s) should continue to move. When all the fingers are blocked, the force should be well-distributed among the fingers and it should be possible to apply large grasping forces while maintaining a stable grasp. Introducing underactuation between the fingers of a robotic hand allows one to reduce the complexity of the systems, from the actuation point of view. As a result, the underactuated grippers require less complex control algorithms, which in turn reduce the need for extensive sensing capabilities and increase reliability in unstructured environments. Aukes *et al.* (2011) describes an underactuated hand mechanism able to adopt a wide range of grasp types by varying the internal forces in its fingers. The adjustment is accomplished by varying the preloads of springs, which affect the grasp stability and stiffness for large and small objects. The problem of optimizing underactuated and passively adaptive robotic hands is discussed in Ciocarlie and Allen (2010).

Due to the multiple degrees of freedom of a single compliant joint, any compliant mechanism (Lu and Kota, 2002, 2003a, b, 2005; Kota *et al.*, 2003; Birglen and Gosselin, 2005; Luo *et al.*, 2005) can be considered as an underactuated mechanism, i.e. with fewer actuators than degrees of mobility. Compliant underactuated grippers show particular promise for use in unstructured environments, where object properties are not known a priori and sensing is prone to error. Finger compliance allows the gripper to passively conform to a wide range of objects while minimizing contact forces. Passive compliance offers additional benefits, particularly in impacts, where control loop delays may lead to poor control of contact forces. Compliance can also lower implementation costs by reducing the sensing and actuation required for the gripper. In article (Steutel *et al.*, 2010), it was designed an underactuated finger with distributed compliance but this mechanism has no adaptability to any unpredictable grasping shapes.

The general principle of the adaptive compliant gripper was introduced in Petković and Pavlović (2012) where the active control system was used to enable gripper accommodation. Since the active system requires controlling a lot of actuators and sensors it was decided to use a passive approach. Therefore, a passive compliant gripper with underactuation is developed in this article. The optimal topology structure of the adaptive gripper is obtained by optimality criteria method using mathematical programming technique (Bendsoe and Sigmund, 2003; Sigmund, 1994, 1997, 2001). The main goal is to obtain a gripper topology structure which behavior will depend only on the external constraints, i.e. contacts with external objects. Additional constraints will be implemented in the optimality criteria method if the obtained gripper structure has any part with concentrated compliance. The main feature of the gripper should lies in its compliant mechanism structure with fully distributed compliance. Compliant mechanisms attain their mobility from flexibility of their constituents as opposed to their rigid body counterparts that attain their mobility from hinges, bearings and sliders. The main advantages of compliant mechanisms are that they can be built using fewer parts or even one part, require fewer assembly processes and need no lubrication. Special care must be taken, however, in designing compliant mechanisms in order to obtain sufficient mobility and safety against failure due to fatigue. One of the most important objectives in compliant mechanism is to be able to control the ratios between output and input displacements or output and input forces which are described by the geometrical and mechanical advantages, respectively. Afterwards, the obtained mechanism structure will be improved by iterative FEM optimization procedure – kinematic approach. The kinematic approach should improve gripper capabilities and grasping as well.

2. Synthesis of compliant finger mechanism using optimality criteria method

Figure 1 shows the two main target functions for the optimization procedure. The place for the unknown mechanism is shown as well as the rigid body counterpart mechanisms for both shapes. Different behavior of the rigid body mechanisms according to the grasping shapes of objects can be seen. For the convex shape, when the gripper makes contact with the input phalange, the last phalange continues to move until the contact with the grasping object. For the concave shape, the gripper at the beginning makes the first contact with the grasping object through the last phalange and afterwards the input phalange continues to move in the input direction, but the upper phalange changes direction until the full accommodation of the grasping object. Only a fully compliant mechanism should enable the adaptable behavior of the gripper.

Topology optimization of compliant mechanisms can be performed based on continuum, as well as truss and frame, discretization. Here, the continuum discretization was used. The goal of the topology optimization problem is to design a structure that converts an input displacement on a prescribed output displacement. To be able to transfer work from the input port to the output port, the displacement must be performed in a structurally efficient way. Here, the gripper contact points with object were assumed fixed.

Assuming that the input is a linear strain based actuator; it can be modeled by a spring with stiffness k_1 and force f_1. The input port has input displacement u_1. The goal of the optimization problem is to maximize output displacement u_2 (or force or work) performed on a workpiece modeled by a spring with stiffness k_2. By specifying different values of k_2 the output displacement amplification can be controlled. If a low value of k_2 is specified, the large output displacements can be obtained and vice versa. In order to maximize the work on the output spring, the available material must be distributed in the structurally most efficient way. The design domain is shown in Figure 2. Here, a unit force (f_1) is applied to the input spring on the right. Therefore, the objective is to maximize the displacement at the output spring (u_2). Since the adjoint method is used to calculate the sensitivity of u_2, it is necessary to use two load cases. This means that F is a matrix with two columns, $F = [F_1, F_2]$, where the first column contains force f_1 that is applied to node n_1 at the input spring, and the second column contains the unit virtual load f_2, applied to

Figure 1 Two different target grasping functions for optimization procedure

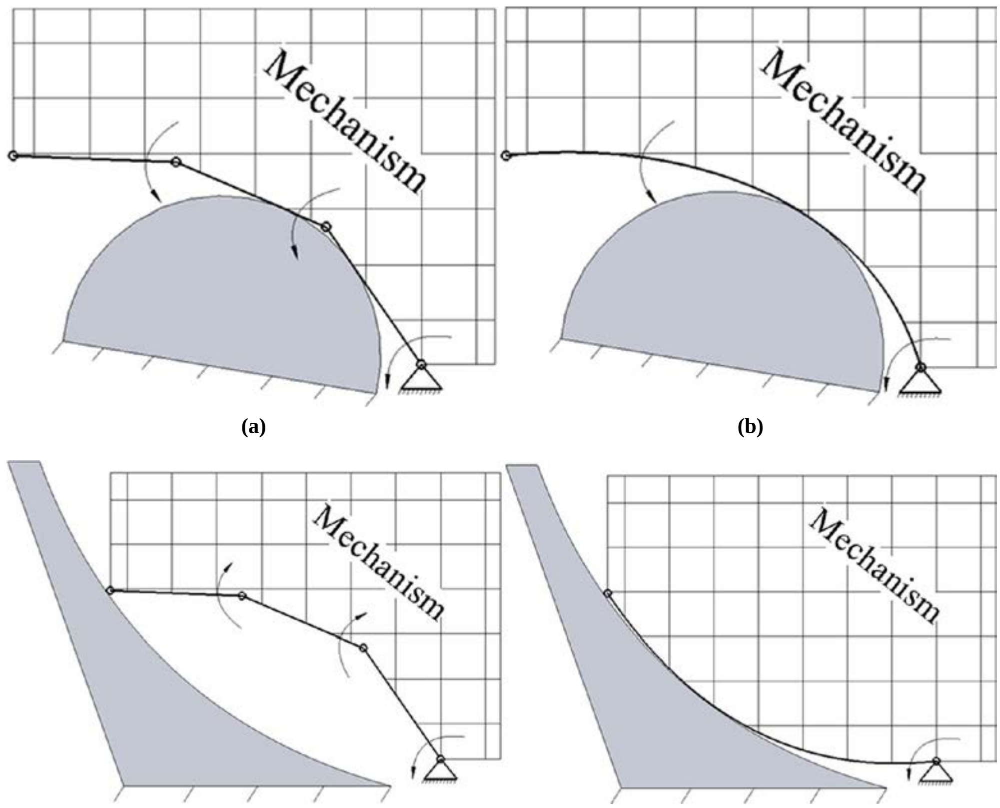

Notes: (a) Rigid body finger behavior for convex grasping shape; (b) compliant finger behavior for convex grasping shape; (c) rigid body finger behavior for concave grasping shape; (d) compliant finger behavior for concave grasping shape

node n_2 at the output spring, which effectively "extracts" the displacement at the output spring. The global displacement matrix also consists of two columns, $U = [U_1, U_2]$. Here, it can be seen that the contact point becomes the support during the optimization process (Figure 2).

Design domain is discretized by square elements and the elements' density was applied as optimization variable (x_i) (Figure 3); modulus of elasticity for an element will be expressed as:

$$E_i = E_0 x_i$$

where E_0 represents real modulus of elasticity.

When variable x_i reaches the smallest value, it can define that the element should be removed from the rest of the structure and this segment becomes void. If several elements in a group reach the smallest density values the large empty space will be created. If element x_i reached the highest density value it will create the optimal mechanism structure. When the density value stays between the two boundaries that it becomes intermediate density. Since it is not suitable to have intermediate values for density the numerical algorithm should decide which is the closest boundary value.

The displacement at the output spring can now be written as:

$$u_{out} = F_2^T U_1$$

and the optimization problem looks as follows:

$$\min_{\underline{x}} : u_{out}(\underline{X}) = F_2^T U_1 = \sum_{e=1}^{N} (\underline{u}^e)^T K^e \underline{u}^e$$

$$= \sum_{e=1}^{N} (x^e)^p (\underline{u}^e)^T K^0 \underline{u}^e \qquad (1)$$

$$\frac{V(\underline{x})}{V_0} \le f$$

$$K\underline{u} = F$$

$$0 < x_{min} < x \le 1$$

$\underline{x}$ is the vector with the densities of all the elements.
$\underline{x}^e$ is the relative density of the material in the element.
$V(\underline{x})$ is the material volume.
V_0 is the design domain volume.
f is the allowable volume fraction.
K is the global stiffness matrix.
$\underline{u}$ is the global displacement vector.
$\underline{K}^e$ are the local elemental stiffness matrices.
K^0 is the local stiffness matrix of an element with a relative density of one.
$p > 1$ is a penalty factor to prevent intermediate densities.
N is the number of elements.
$\underline{u}^e$ is the local displacement vector.

Figure 2 Design domains of the finger mechanism optimization process for two grasping shapes of object – concave (a) and convex (b)

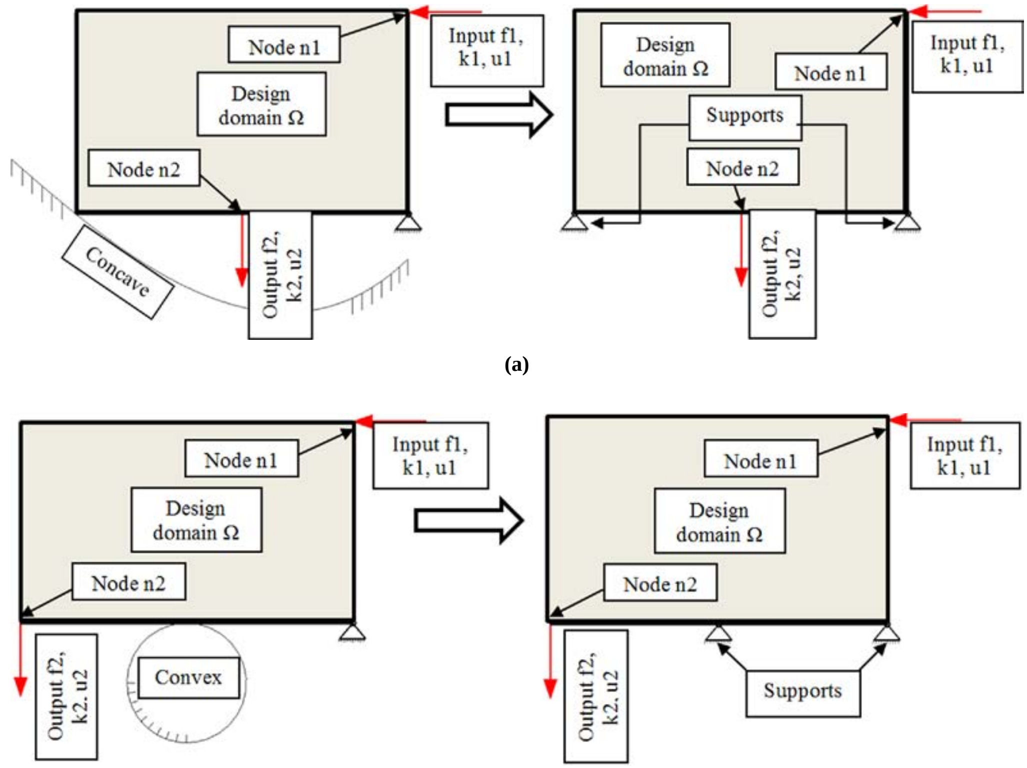

(a)

(b)

Figure 3 Design domain discretization by density elements; optimization variable is element density (a) and possible topology structure for a compliant mechanism (b)

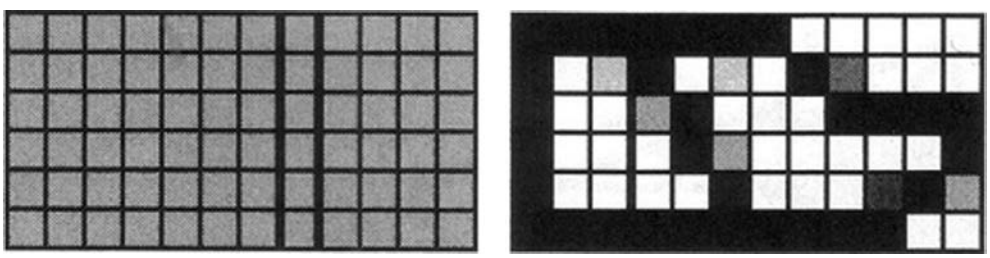

(a) (b)

The values of x^e are allowed to vary between x_{min} and $x = 1$ to relax the problem formulation, but the final design should consist of only solid and void elements.

The optimization problem (1) is solved using the optimality criteria updating scheme. The Lagrangian for the optimization problem can be written as:

$$L = u_{out} + \lambda(V(\underline{x}) - fV_0) + \underline{\lambda}_1^T(K\underline{u} - F) + \sum_{e=1}^{N} \lambda_2^T(x_{min} - x^e)$$

$$+ \sum_{e=1}^{N} \lambda_3^T(x^e - x_{min})$$

where λ_i are the Lagrangian multipliers. Optimality is found when the derivatives of the Lagrangian with respect to the design variables are zero:

$$\frac{\partial L}{\partial x^e} = 0, \quad 3a \quad e = 1, \ldots, N,$$

$$\frac{\partial L}{\partial x^e} = \frac{\partial u_{out}}{\partial x^e} + \lambda \frac{\partial V(\underline{x})}{\partial x^e} + \underline{\lambda}_1^T \frac{\partial (K\underline{u})}{\partial x^e} - \lambda_2^e + \lambda_3^e$$

Assuming that the upper- and lower-bound constraints are not active $\left(\lambda_2^e = \lambda_3^e = 0\right)$ and that the loads are design independent $((\partial F/\partial x^e) = 0)$, the derivative of the Lagrangian can be written as:

$$\frac{\partial L}{\partial x^e} = \underline{u}^T \frac{\partial K}{\partial x^e} \underline{u} + \underline{\lambda}_1^T \frac{\partial K}{\partial x^e} \underline{u} + \frac{\partial u}{\partial x^e}(2\underline{u}^T K + \underline{\lambda}_1^T K) + \lambda V^e \quad (2)$$

Since $V(\underline{x}) \approx \underline{x}^T \underline{v}$, with $\underline{v}$ the column with all the element volumes, the sensitivity of $V(\underline{x})$ with respect to the design variable can be written as:

$$\frac{\partial V(\underline{x})}{\partial x^e} = V^e$$

With V^e the volume of element e. Since $\underline{\lambda}_1^T$ in equation (2) is arbitrary and to eliminate $\partial u/\partial x^e$, $\underline{\lambda}_1^T$ is chosen as $-2\underline{u}^{\mathrm{T}}$. Now, the derivative of the Lagrangian is:

$$\frac{\partial L}{\partial x^e} = -\underline{u}^T \frac{\partial K}{\partial x^e}\underline{u} + \lambda V^e = -p(x^e)^{p-1}(\underline{u}^e)^T K^0 \underline{u}^e + \lambda V^e = 0$$

The design variables can now be updated using:

$$\frac{p(x^e)^{p-1}(\underline{u}^e)^T K^0 \underline{u}^e}{\lambda V^e} = \frac{(\partial \mathrm{u_{out}}/\partial x^e)}{\lambda V^e} = B_k^e = 1$$

$$x_{k+1}^e = B_k^e x_k^e$$

To prevent x from changing too much in one iteration, a moving limit m is introduced. The heuristic updating scheme can now be formulated as (Bendsoe, 1995):

$$\mathrm{x}_{k+1}^{e} = \begin{cases} \max\left(\mathrm{x_{min}}, \mathrm{x}_k^e - \mathrm{m}\right) & \text{if } \mathrm{x}_k^e\left(\mathrm{B}_k^e\right)^{\eta} \leq \max\left(\mathrm{x_{min}}, \mathrm{x}_k^e - \mathrm{m}\right) \\ \mathrm{x}_k^e\left(\mathrm{B}_k^e\right)^{\eta} & \text{if } \max\left(\mathrm{x_{min}}, \mathrm{x}_k^e - \mathrm{m}\right) \leq \mathrm{x}_k^e\left(\mathrm{B}_k^e\right)^{\eta} \leq \min\left(1, \mathrm{x}_k^e + \mathrm{m}\right) \\ \min\left(1, \mathrm{x}_k^e + \mathrm{m}\right) & \text{if } \mathrm{x}_k^e\left(\mathrm{B}_k^e\right)^{\eta} \geq \min\left(1, \mathrm{x}_k^e + \mathrm{m}\right) \end{cases}$$

where $\eta(=0.05)$ is a numerical damping coefficient to stabilize the iteration. The value of the Lagrangian multiplier λ can be found by a bisection algorithm.

The optimal finger structure topology obtained by optimality criteria method is shown in Figure 4. The finite element discretization was 60×40 and volume fraction was 0.5. Here can be seen that the obtained gripper structure has fully compliance so it is need to implement additional constrains in the optimization procedure. The finger verification is shown in Figure 5 for both grasping shapes, convex (a) and concave (b). It can be noted that the gripper behavior depends on contact point positions.

3. FEM iterative optimization procedure – kinematic approach

Figure 6 shows the input mechanism principle for one finger. As it is shown in Figure 1(a) the basic input mechanism for the finger can be presented as a slider crank mechanism. Figure 1(b) shows the slider crank mechanism with the addition of the finger design domain. FEM iterative optimization procedure should optimize finger design topology and input mechanism as well.

To investigate the behavior of the fully compliant underactuated adaptive gripper, many FEM simulations were performed. As an initial gripper topology structure, multi-finger gripper with two fingers was chosen. Additionally, each of the fingers has three phalanges in the initial stage. The number of phalanges was increased to cover and investigate all possible solutions of the gripper structure. The number of the finger phalanges represent optimization variable as well. Figure 7 shows the initial gripper topology and all optimization parameters which were altered during the optimization process. The initial gripper topology was obtained according to the current gripper models from literature (Arimoto, 2004; Birglen, 2011; Bendsoe and Sigmund, 2003; Bendsoe, 1995). The FEM simulations were made to determine and verify the design of the gripper for two target grasping functions, to grasp the objects of concave and convex shape objects. Besides, the accommodation of the gripper to many other shapes of grasping objects was verified. The cylindrical grasping objects with radius r = 5 mm, r = 7.5 mm, r = 10 mm, r = 12.5 mm, r = 15 mm and r = 20 mm were mostly used for the optimization procedure but many other grasping shapes were also used like cubic, conic, triangular, parallelepiped and, etc.

Some optimization parameters were unchangeable, while some parameters depended on other parameters. The entire FEM analysis was performed in ABAQUS software with following parameters and characteristics:

- grasping object as explicit discrete rigid element;
- finite element type for grasping object R3D4: a 4-node 3D bilinear rigid quadrilateral, 1 mm size;
- gripper material: silicone rubber (*Elastosil R420/70 MH E*);
- solid and homogeneous section for the gripper;
- gripper as explicit 3D stress element; and
- finite element type for the gripper C3D8R: an 8-node linear brick, reduced integration, hourglass control, 1 mm size (Table I).

The final solution of adaptive compliant gripper with passive compliance and underactuation was designed with two fingers and one input port as shown in Figure 8. This figure depicts fixed and input ports as well. It can be noticed that the gripper model was designed entirely as one part. Gripper height can be also noticed in Figure 8.

Figure 9 shows the main working principle of the gripper with two fingers. The two-fingered gripper has one common input and the each finger has independent accommodation and movement. As the main parameter for the gripper accommodation inspection, gripper tip displacement in *x*-direction was chosen as it shown in Figure 9.

Figure 10 shows the optimal finger topology obtained by FEM iterative optimization procedure. This structure was tested for two main target functions as it shown in Figure 11(a)

Figure 4 Optimal design for the gripping mechanism obtained by optimality criteria method

Industrial Robot: An International Journal
Volume 40 · Number 6 · 2013 · 610–623

Figure 5 Deflections of the optimal finger mechanism for convex (a) and concave grasping shapes (b)

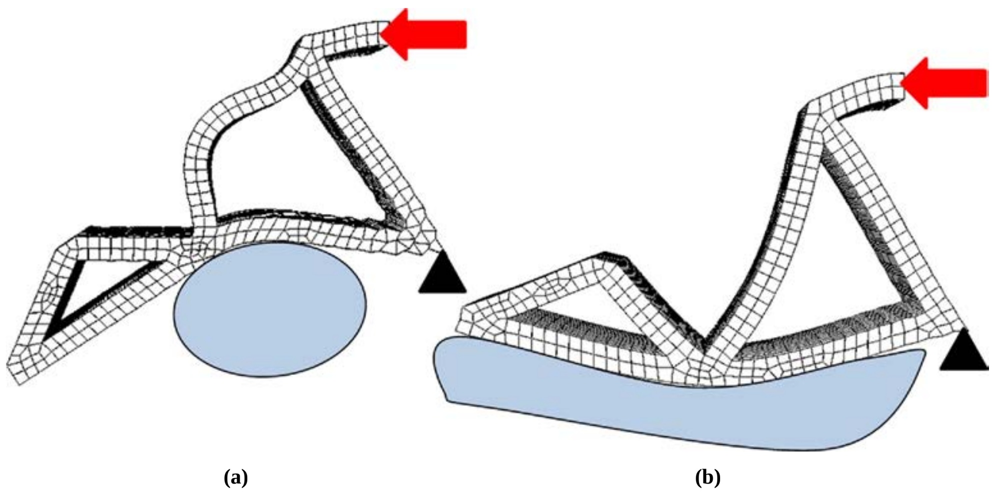

Figure 6 Input mechanism for on finger as (a) slider crank mechanism and (b) finger design domain

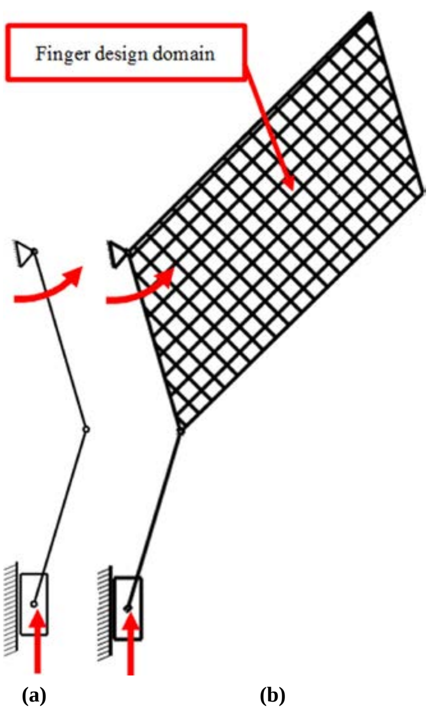

for convex and in Figure 11(b) for concave grasping shape of object.

4. FEM simulation and testing

Many FEM simulations were performed to verify the gripper behavior for any grasping shape of the objects. Figure 12 shows the verification of the gripper behavior for seven different shapes and sizes of the grasping objects. It can be noticed that the grasping object could be asymmetric as well.

After the optimization process small modifications of the gripper structure were performed according to manufacturing

Figure 7 Initial gripper structure with all optimization parameters for FEM optimization procedure

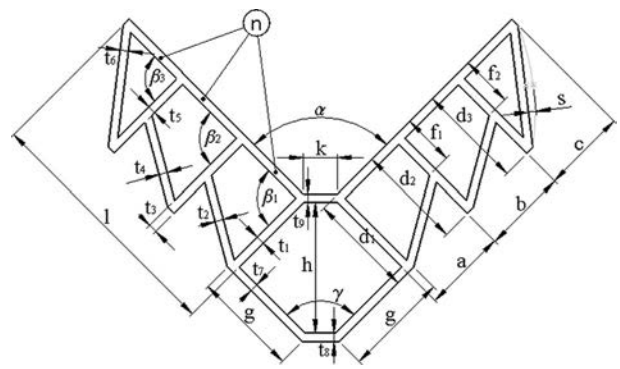

requirements. Figure 13 shows the main features of the two-fingered gripper. These are:

- the whole gripper structure represents one passive elastic structure (Figure 13(a));
- for one active input, the gripper has multi-output contact points (Figure 13(b)); and
- one active input actuator (Figure 13(b)).

The gripper part which is fixed during gripping and holding of a grasped object is shown as well. The gripper accommodation to the cylindrical object with the radius r = 25 mm can be noticed in Figure 13(b).

As it noted already, silicone rubber *Elastosil R420/70 MH E* was used for gripper manufacturing. Before FEM simulation of the gripper with this material was performed, it was need to acquire experimental strain-stress relationships according to *ASTM D575* standard for unaxial rubber testing to use the real material for FEM simulations.

Figure 14(a) shows gripper maximal stress changing while grasping of cylindrical object with radius r = 50 mm. As can be seen, the relationship is almost linear in relation to input displacement. The maximal stress in the gripper structure is 0.4 Mpa at the end of grasping process. Relationship of the maximal contact pressure in relation to input displacement is shown in Figure 14(b). This graph shows that the maximal

Industrial Robot: An International Journal
Volume 40 · Number 6 · 2013 · 610–623

Table I Optimization parameters for FEM iterative optimization procedure

	Optimization parameters			
Parameters	Range	Initial value	Optimal value	Increment
α	$60 \leq \alpha \leq 120$	$\alpha_0 = 90°$	$\alpha = 90°$	
β1	$90 \leq \beta_1 \leq 120$	$\beta_{10} = 90°$	$\beta_1 = 120°$	10
β2	$90 \leq \beta_2 \leq 120$	$\beta_{20} = 90°$	$\beta_2 = 120°$	10
β3	$90 \leq \beta_3 \leq 120$	$\beta_{30} = 90°$	$\beta_3 = 120°$	10
γ	$25 \leq \gamma \leq 90$	$\gamma_0 = 90°$	$\gamma = 25°$	
a	$20 \leq a \leq 20$	$a_0 = 20$	$a = 20$	
b	$20 \leq b \leq 20$	$b_0 = 20$	$b = 20$	
c	$20 \leq c \leq 20$	$c_0 = 20$	$c = 0$	5
d1	$25 \leq d_1 \leq 25$	$d_{10} = 25$	$d_1 = 25$	
d2	$5 \leq d_2 \leq 25$	$d_{20} = 25$	$d_2 = 5$	5
d3	$0 \leq d_3 \leq 25$	$d_{30} = 25$	$d_3 = 0$	5
f1	$0 \leq f_1 \leq 25$	$f_{10} = 25$	$f_1 = 5$	5
f2	$0 \leq f_2 \leq 25$	$f_{20} = 25$	$f_2 = 0$	5
t1	$2 \leq t_1 \leq 4$	$t_{10} = 2$	$t_1 = 2$	1
t2	$2 \leq t_2 \leq 4$	$t_{20} = 2$	$t_2 = 2, t_2 = 3$	1
t3	$2 \leq t_3 \leq 4$	$t_{30} = 2$	$t_3 = 2$	1
t4	$2 \leq t_4 \leq 4$	$t_{40} = 2$	$t_4 = 2$	1
t5	$2 \leq t_5 \leq 2$	$t_{50} = 2$	$t_5 = 2$	
t6	$2 \leq t_6 \leq 2$	$t_{60} = 2$	$t_6 = 2$	
t7	$2 \leq t_7 \leq 5$	$t_{70} = 2$	$t_7 = 5$	3
t8	$2 \leq t_8 \leq 20$	$t_{80} = 2$	$t_8 = 20$	18
t9	$0 \leq t_9 \leq 2$	$t_{90} = 2$	$t_9 = 2$	2
s	$0 \leq s \leq 2$	$s_0 = 0$	$s = 0$	1
l	$60 \leq l \leq 60$	$l_0 = 60$	$l = 60$	
k	$0 \leq k \leq 8$	$k_0 = 0$	$k = 4$	2
h	$30 \leq h \leq 50$	$h_0 = 30$	$h = 50$	10
g	$20 \leq g \leq 40$	$g_0 = 25$	$g = 20$	
n	$2 \leq n \leq 3$	$n_0 = 3$	$n = 2$	2

Source: Osswald *et al.* (2004)

Figure 8 Compliant gripping mechanism with two optimal fingers and one input port

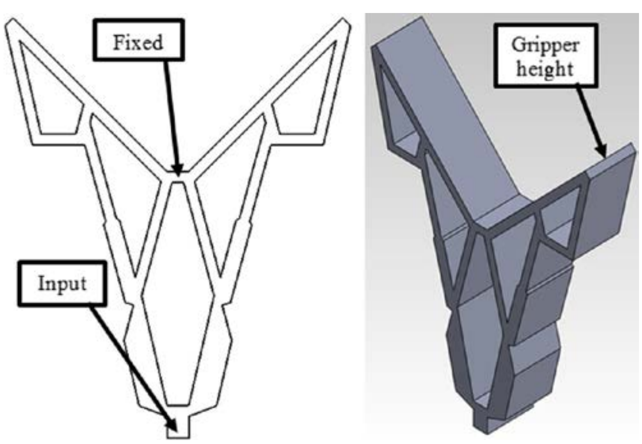

contact stress increases until 17 mm of input displacement. Afterwards, the graph is almost constant until approximately 30 mm of input displacement. The reason for that might be in separation of gripper contact surfaces from grasping object. A drastic increase of the maximal contact pressure occurred after approximately 35 mm of input displacement. The maximal contact pressure is 0.025 Mpa which is especially suitable for sensitive and fragile grasping objects. Taken together, these results provide support for the model concerning sensitive grasping objects, since the goal was to eliminate the part of the drastic increase in the contact pressure. The graphs were obtained in ABAQUS software for FEM simulations.

Figure 15 shows gripper tip displacement during grasping process – solid line. The displacement in *x*-direction is shown as well – dashed line. By analyzing the graphs it was clear that the mainly displacement of the gripper tip was in *x*-direction for the cylindrical object. The graphs were obtained in ABAQUS software for FEM simulations.

Figure 16 shows maximal contact pressures changing in relation to input displacement for the both fingers separately. It can be noticed that the maximal contact pressures on the contact surface of the both fingers were not the same. Maximal contact pressure was 0.04 MPa on the right contact surfaces. The graphs were obtained in ABAQUS software for FEM simulations.

By analyzing the changing of contact forces in relation to input displacement (Figures 17 and 18) for the both finger separately it can be concluded that the contact forces are the same. Additionally, it is also shown the contact forces in the *x*-direction. It is clear that the contact forces mainly act in *x*-direction. The graphs were obtained in ABAQUS software for FEM simulations.

The relationship between the input displacement and the total area in contact for the both finger is shown in Figure 19. It is interesting to note that the area in contact decreased after approximately 25 mm of input displacement. The result indicates that there was a separation between the gripper surfaces and the grasping object at approximately half of the input displacement since there is drastic decrease of the total area in contact. The graphs were obtained in ABAQUS software for FEM simulations.

5. Gripper manufacturing

The complete gripper manufacturing process is presented in Issa *et al.* (2011). The moulding tool for the gripper manufacturing is shown in Figure 20. The process follows the next steps:

- the tool cavities are filled with raw carbon-black filled silicone rubber; and
- press-curing at T = 180°C and pressure of p = 26 kN for about 30 min.

The extracted gripper from the tool is shown as well. In future research, the sensors will be made of conductive silicone rubber which will be more elastic than silicone rubber for the gripper structure to ensure more deformation in the sensors. This paper explains the production of the gripper structure without a sensor. In the beginning, silicone rubber with different shore hardness was used, i.e. 60, 70 and 80. According to the experimental test, the best silicone shore hardness was 70 and, therefore, Elastosil R420/70 was used. Higher silicone shore hardness than 70 leads to the very stiff gripper structure which could not achieve adaptation to the grasping objects. On the other hand, lower silicone shore hardness than 70 leads to the very soft gripper structure which could not achieve adaptation to the grasping objects because the main condition for the good gripper adaptivity is flexibility of the gripper structure. The FEM simulations were proven by testing the adaptable behavior of the produced gripper. It should be noted that the gripper accommodation could be

Figure 9 The main working principle of the gripper

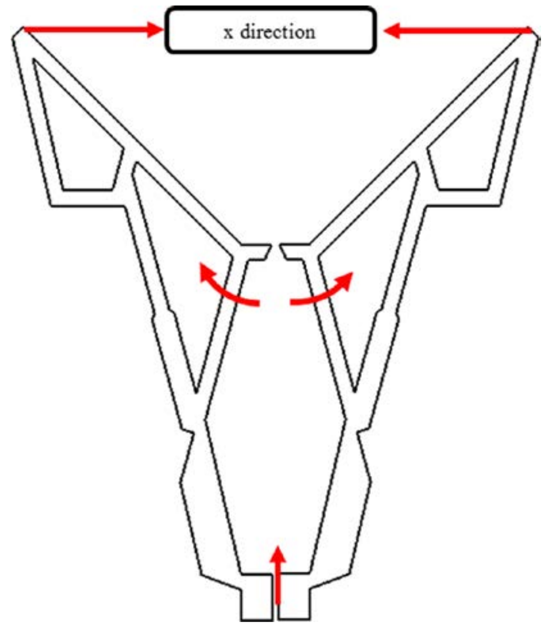

Figure 10 Optimal design for the finger mechanism obtained by FEM iterative method

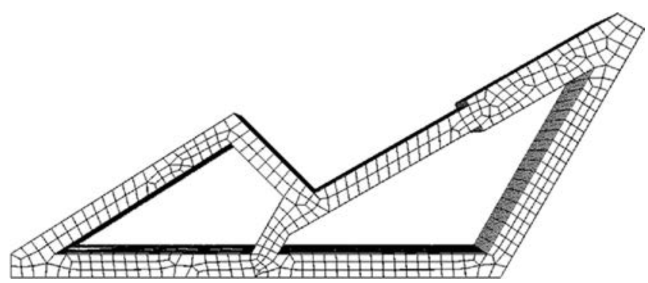

Figure 11 Deflections of the optimal finger mechanism for convex (a) and concave shapes (b)

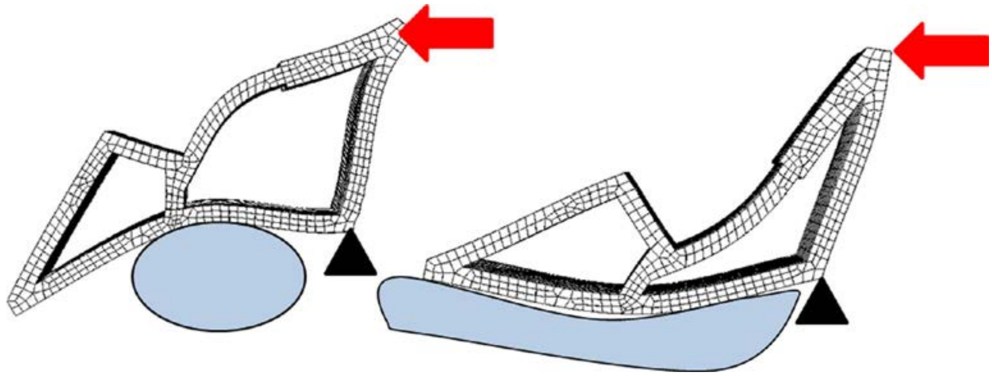

performed without fixing any part of the gripper structure, i.e. the gripper could be forced into the grasping object. On the other hand the gripper could be fixed at the fixed node and the gripper input node would be pulled to the fixed node. Here LabVIEW virtual instrument and National Instruments BNC-2120 card were used for the gripper displacement control and Zwick ProLine material-testing machine Z005 was used for the gripper actuation (Issa *et al.*, 2011).

Figure 12 Verification of the two-fingered gripper functions for different shapes and sizes of grasping objects

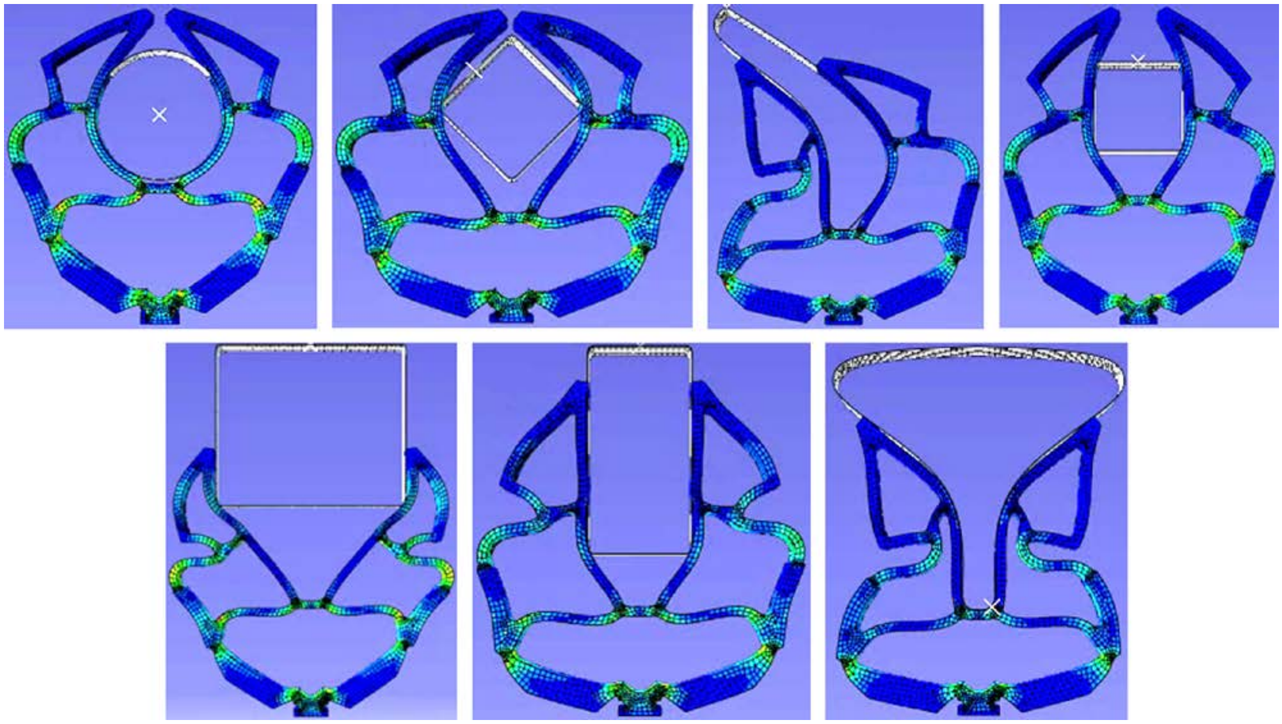

Figure 13 The main features of the passive adaptive gripper

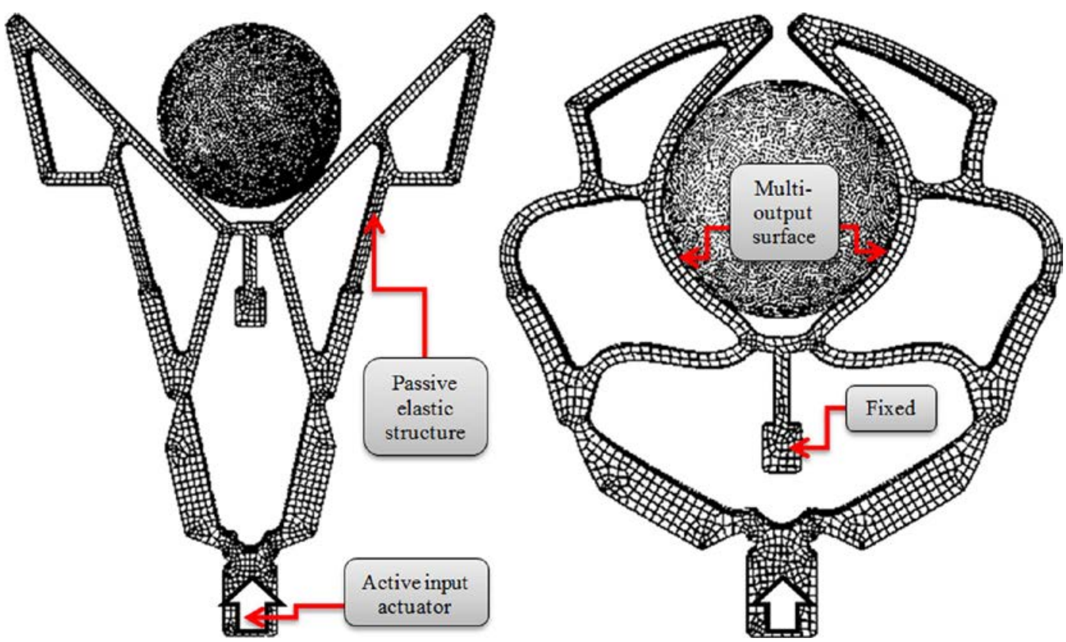

6. Discussion

The two-fingered gripper structure can be useful for experimental analysis of the finger characteristics. Although, for real grasping applications in robotics, two-fingered grippers could show unstable behavior during grasping and holding the objects. For such a purpose, it is useful to model multi-fingered grippers with three or more fingers. Figure 21(a) shows three-fingered gripper accommodation to the spherical object (convex grasping shape). Figure 21(b) shows four-fingered gripper accommodation to the spherical grasping object. In both cases, single actuation principle was used. It means that with one actuator and without any control procedure the gripper should provide safe and fully

Figure 14 Relationship between input displacement and maximal gripper structure stress (a) and maximal contact pressure (b) for the gripper height 8 mm

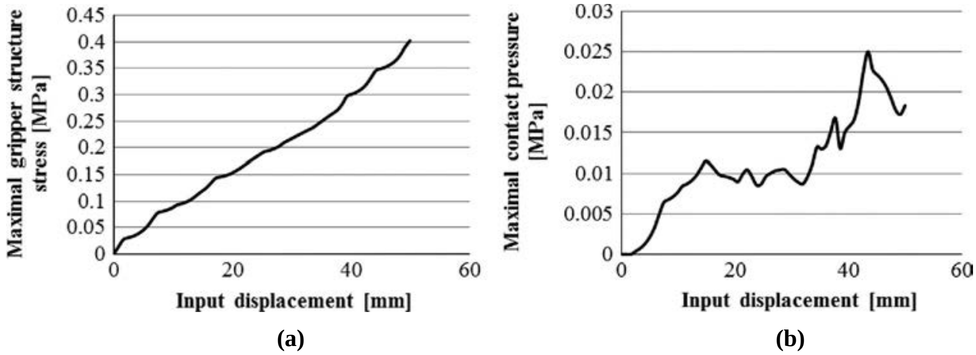

Figure 15 Gripper tip displacement in relation to input displacement

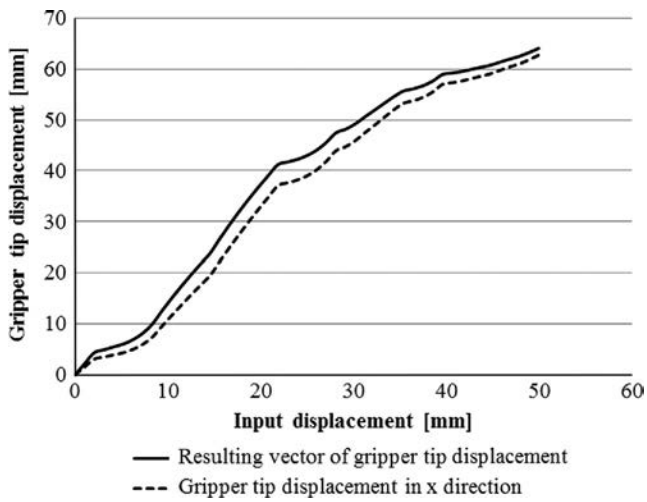

Figure 16 Maximal contact pressure changing on the both fingers separately in relation to input displacement for the gripper height 8 mm

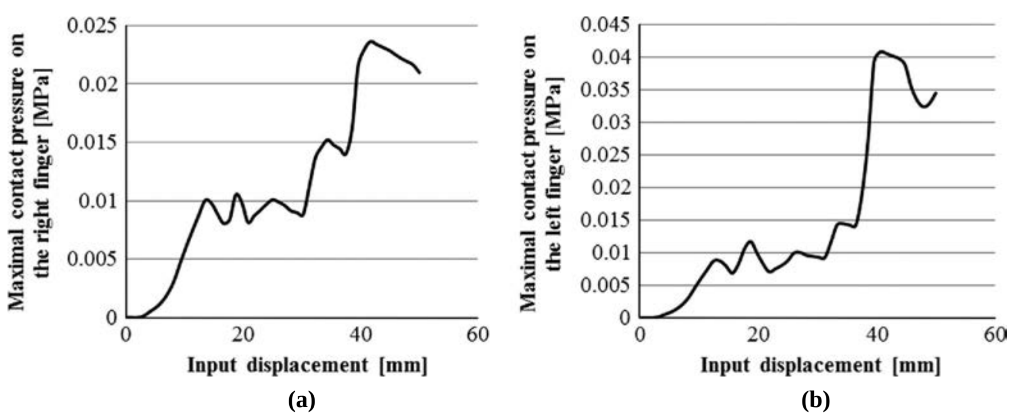

accommodation to the object. This is the main advantage of the passive mechanisms with underactuation.

To improve behavior of the gripper in regard on its flexibility and fragility it is recommended to increase gripper height (Figure 22) for industrial applications. Such a gripper could be useful for manipulation with sensitive and soft object to avoid any damage of the grasping objects.

An important question arises concerning the development of the adaptive robotic gripper. The question can be stated as: "Is active control needed to perfectly mimic the human hand

Figure 17 Contact force changing on the left finger in relation to input displacement

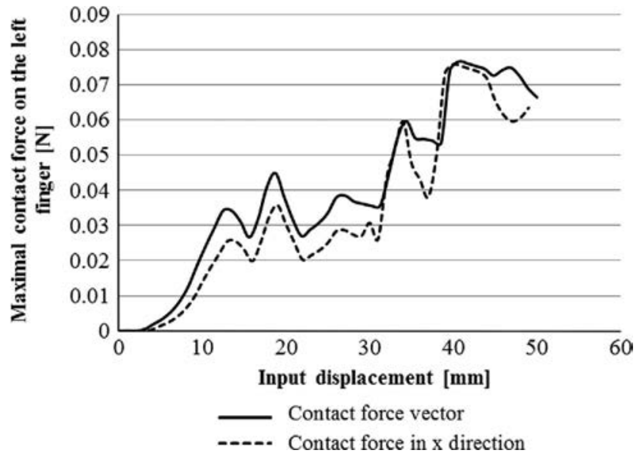

Figure 18 Contact force changing on the right finger in relation to input displacement

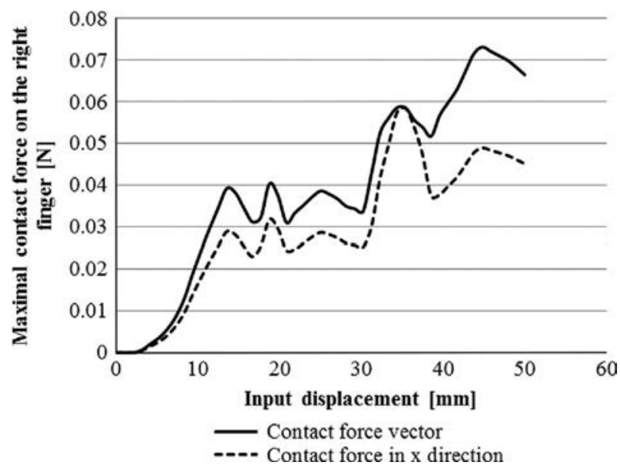

Figure 19 Total area in contact changing for the both finger separately

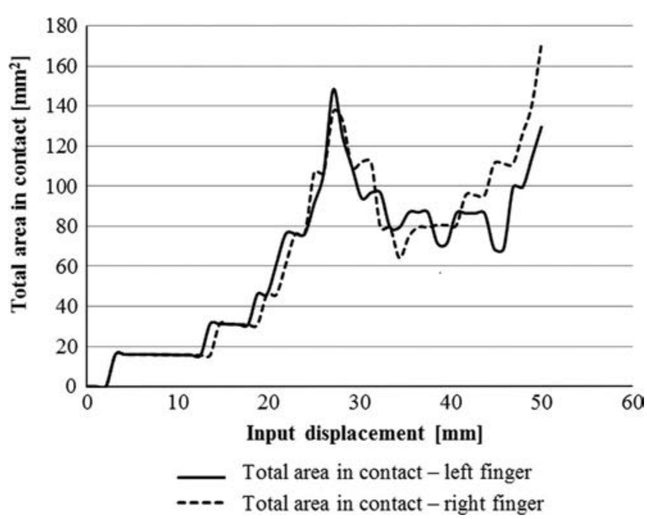

Figure 20 The moulding tool for gripper manufacturing (a), extracted gripper (b), and gripper testing (c)

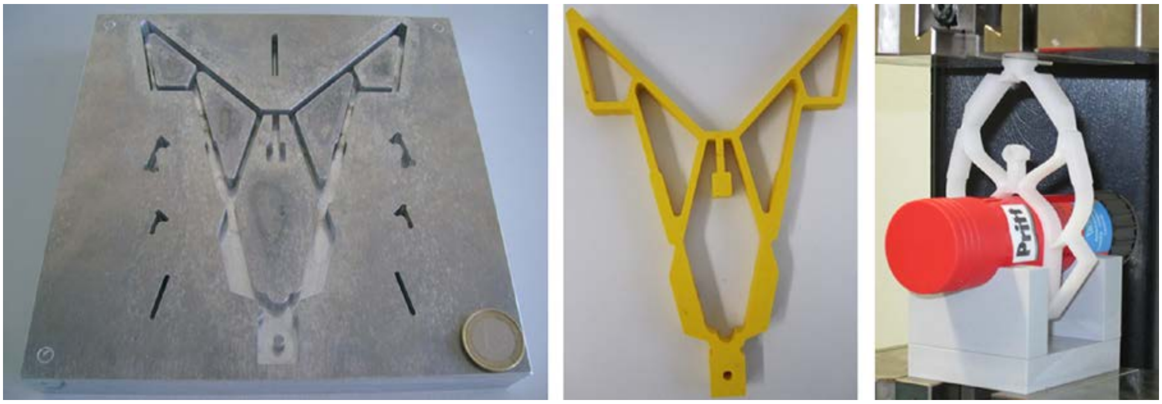

(a) **(b)** **(c)**

Figure 21 The multi-fingered grippers with: (a) three fingers and (b) four fingers

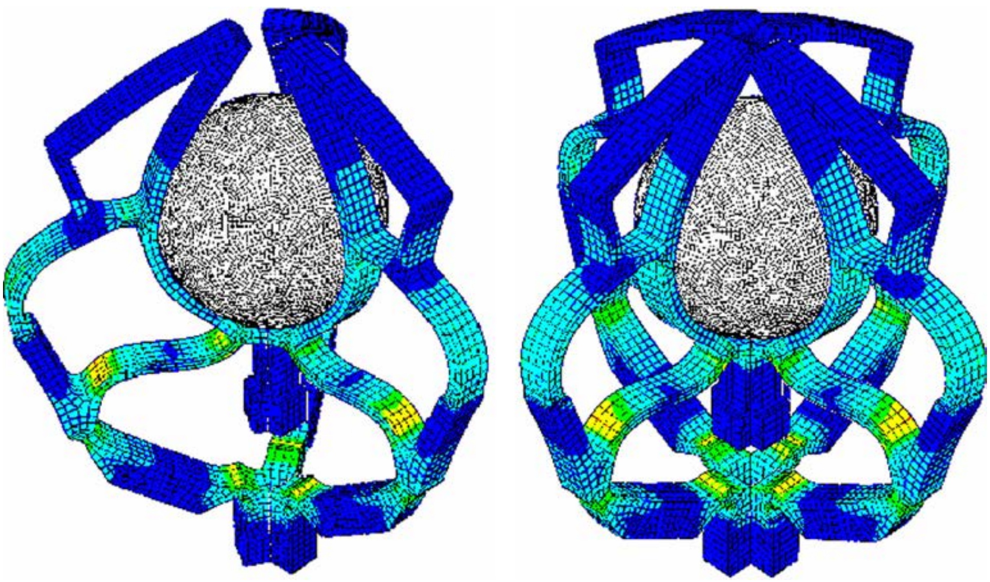

(a) **(b)**

adaptation, or is as simple mechanical design with approximate adaptive grasp sufficient?" The question itself illustrates the difference in design strategies between active (computer controlled) adaptive grasp (Osswald *et al.*, 2004; Arimoto, 2004; Yoshikawa, 2010) and passive (mechanism control) adaptive grasp (Carrozza *et al.*, 2004; Montambault and Gosselin, 2001; Fukaya *et al.*, 2000). The gripper must implement three mechanical features that together give it the ability for passive adaptive grasp. First, the fingers must be able to curl as they closing around the grasping object. Second, the fingers must be able to closing around the grasping object independently of each other during grasping. Finally, the fingers must be able to rotate inwards and rotate outwards as well as to closing around the grasping object and opening around the grasping object.

7. Conclusion

The handling of irregular, unpredictably shaped and sensitive objects introduces demands on gripper flexibility and dexterity. Reaching the dexterity and adaptation capabilities requires the control of a lot of actuators and sensors. The dexterity can also be obtained by underactuation, which consists in equipping the finger with fewer actuators than the number of degrees of freedom. Here, gripper was equipped with one active controllable actuator which enables gripper accommodation to any irregular object. To simplify analysis two grasping shapes were emphasized, concave grasping shape and convex grasping shape. Another advance of the gripper was its fully flexibility. The flexibility can be reached by introducing compliant mechanisms with distributed compliance, i.e. fully compliant mechanisms. The combination of the underactuation and

Figure 22 Increased gripper height

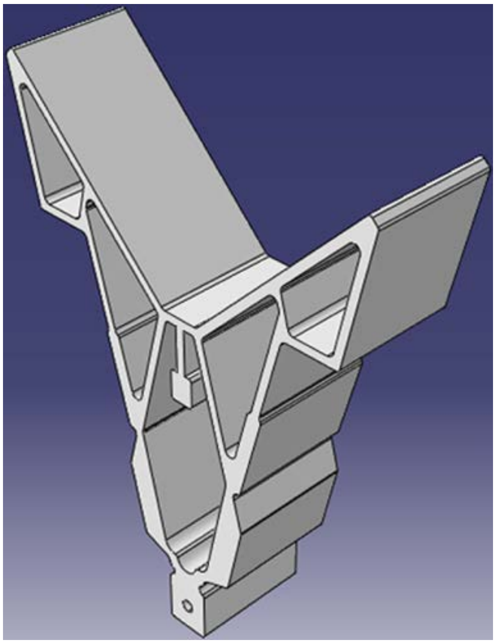

the compliant mechanisms leads to a gripper with high adaptability and sensibility. Another characteristic of compliant underactuated grippers is the elasticity of the silicon rubber which ensures a soft contact between the gripper and the grasped object, e.g. sensitive grasping.

The gripper method utilized here is a new and original principle for adaptive grasping. The main difference between this design and previously established grippers lies in its distributed compliance, gripper structure as one part, simple manufacturing process, low cost and easy adaptation to any irregular object. It should be emphasized that the gripper structure has very large deformations and the gripper could be used in macro and in micro domain as well. In other words, the gripper structure has not displacement limitations. The behavior of the gripper depends only on contact points positions with external objects. In other words the gripper has passive adaptability feature. The only drawback of this gripper lies in its very high flexibility, i.e. it is not able to hold heavy objects. One of the solutions to handle this problem is to increase the height of the gripper. Another solution is to use grippers with more fingers, three or more fingers. Also, the gripping contact forces are very small and it ensures soft contacts during grasping.

References

Arimoto, S. (2004), "Intelligent control of multi-fingered hands", *Annual Reviews in Control*, Vol. 28, pp. 75-85.

Aukes, D., Heyneman, B., Duchaine, V. and Cutkosky, M.R. (2011), "Varying spring preloads to select grasp strategies in an adaptive hand", *IEEE IROS 2011, San Francisco, CA, September*, pp. 1-6.

Bendsoe, M.P. (1995), *Optimization of Structural Topology, Shape and Material*, Springer, New York, NY.

Bendsoe, M.P. and Sigmund, O. (2003), *Topology Optimization, Theory, Methods and Applications*, Springer, Berlin.

Birglen, L. (2011), "The kinematic preshaping of triggered self-adaptive linkage-driven robotic", *Fingers, Mechanical Science*, Vol. 2, pp. 41-49.

Birglen, L. and Gosselin, C.M. (2005), "Fuzzy enhanced control of an underactuated finger using tactile and position sensors", *Proceedings of the 2005 IEEE International Conference on Robotics and Automation*, pp. 2320-2325.

Birglen, L., Laliberté, T. and Gosselin, C.M. (2008), "Underactuated robotic hands", *Springer Tracts in Advanced Robotics*, Vol. 40, p. 244.

Carrozza, M.C., Suppo, C., Sebastiani, F., Massa, B., Vecchi, F., Lazzarini, R., Cutkosky, M.R. and Dario, P. (2004), "The SPRING hand: development of a self-adaptive prosthesis for restoring natural grasping", *Autonomous Robots*, Vol. 16, pp. 125-141.

Ciocarlie, M. and Allen, P. (2010), "Data-driven optimization for underactuated robotic hands", *2010 IEEE International Conference on Robotics and Automation*, pp. 1292-1299.

Doria, M. and Birglen, L. (2009), "Design of an underactuated compliant gripper for surgery using nitinol", *Journal of Medical Devices*, Vol. 3 No. 1.

Fukaya, N., Toyama, S., Asfour, T., Dillmann, R., Montambault, S. and Gosselin, C.M. (2000), "Design of the TUAT/Karlsruhe humanoid hand", *2000 IEEE/RSJ International Conference on Intelligent Robots and Systems*, pp. 1754-1759.

Issa, M., Petković, D., Pavlović, N.D. and Zentner, L. (2011), "Embedded-sensing elements made of conductive silicone rubber for compliant robotic joint", paper presented at 56th Internationales Wissenschaftliches Kolloquium TU Ilmenau (CD-ROM), Ilmenau, Paper Id 1231.

Kota, S., Hetrick, J., Osborn, R., Paul, D., Pendleton, E., Flick, P. and Tilmann, C. (2003), "Design and application of compliant mechanisms for morphing aircraft structures", *Smart Struct. and Materials*, Vol. 5054, pp. 24-33.

Lu, K.-J. and Kota, S. (2002), "Compliant mechanism synthesis for shape-change applications: preliminary results", *Smart Struct. and Materials*, Vol. 4693, pp. 161-172.

Lu, K.-J. and Kota, S. (2003a), "Design of compliant mechanisms for morphing structural shapes", *J. of Intelligent Material and Struct.*, Vol. 14, pp. 379-391.

Lu, K.-J. and Kota, S. (2003b), "Parametrization strategy for optimization of shape morphing compliant mechanisms using load path representation", *Proceedings of DETC'03 ASME 2003 Design Engineering Technical Conferences and Computers and Information in Engineering Conference Chicago, IL, USA*, pp. 693-702.

Lu, K.-J. and Kota, S. (2005), "An effective method of synthesizing compliant adaptive structures using load path representation", *J. of Intelligent Material Syst. and Struct.*, Vol. 16, pp. 307-317.

Luo, M., Lu, C., Mei, T. and Zha, S. (2005), "Intelligent grasping of an underactuated hand for space robots", *Proc. of the 8th International Symposium on Artificial Intelligence, Robotics and Automation in Space – iSAIRAS*, pp. 1-6.

Montambault, S. and Gosselin, C.M. (2001), "Analysis of underactuated mechanical grippers", *Journal of Mechanical Design*, Vol. 123, pp. 367-374.

Osswald, D., Martin, J., Burghart, C., Mikut, R., Worn, H. and Bretthauer, G. (2004), "Integrating a flexible anthropomorphic, robot hand into the control, system of a humanoid robot", *Robotics and Autonomous Systems*, Vol. 48, pp. 213-221.

Petković, D. and Pavlović, N.D. (2012), "A new principle of adaptive compliant gripper, mechanisms, transmission and applications", *Mechanisms and Machine Science*, Vol. 3, pp. 145-152.
Sigmund, O. (1994), "Design of material structures using topology optimization", PhD thesis, Technical University of Denmark, Lyngby.
Sigmund, O. (1997), "On the design of compliant mechanisms using topology optimization", *Mech. Struct. Mach.*, Vol. 25, pp. 495-526.
Sigmund, O. (2001), "A 99 line topology optimization code written in Matlab", *Struct. Multidisc. Optim.*, Vol. 21, pp. 12 and 127.
Steutel, P., Kragten, G.A. and Herder, J.L. (2010), "Design of a fully compliant under-actuated finger with a monolithic structure and distributed compliance", *Proceedings of IDETC/CIE 2010, ASME 2010 International Engineering Technical Conferences & Computers and Information in Engineering Conference 2010*.
Yoshikawa, T. (2010), "Multifingered robot hands: control for grasping and manipulation", *Annual Reviews in Control*, Vol. 34, pp. 199-208.

Corresponding author

Dalibor Petković can be contacted at: dalibortc@gmail.com